

Retraction

Retracted: Iris Localization Algorithm based on Effective Area

International Journal of Antennas and Propagation

Received 23 January 2024; Accepted 23 January 2024; Published 24 January 2024

Copyright © 2024 International Journal of Antennas and Propagation. This is an open access article distributed under the Creative Commons Attribution License, which permits unrestricted use, distribution, and reproduction in any medium, provided the original work is properly cited.

This article has been retracted by Hindawi following an investigation undertaken by the publisher [1]. This investigation has uncovered evidence of one or more of the following indicators of systematic manipulation of the publication process:

- (1) Discrepancies in scope
- (2) Discrepancies in the description of the research reported
- (3) Discrepancies between the availability of data and the research described
- (4) Inappropriate citations
- (5) Incoherent, meaningless and/or irrelevant content included in the article
- (6) Manipulated or compromised peer review

The presence of these indicators undermines our confidence in the integrity of the article's content and we cannot, therefore, vouch for its reliability. Please note that this notice is intended solely to alert readers that the content of this article is unreliable. We have not investigated whether authors were aware of or involved in the systematic manipulation of the publication process.

Wiley and Hindawi regrets that the usual quality checks did not identify these issues before publication and have since put additional measures in place to safeguard research integrity.

We wish to credit our own Research Integrity and Research Publishing teams and anonymous and named external researchers and research integrity experts for contributing to this investigation.

The corresponding author, as the representative of all authors, has been given the opportunity to register their agreement or disagreement to this retraction. We have kept a record of any response received.

References

- [1] J. Yu, L. Zhang, and Z. Wang, "Iris Localization Algorithm based on Effective Area," *International Journal of Antennas and Propagation*, vol. 2021, Article ID 2049646, 11 pages, 2021.

Research Article

Iris Localization Algorithm based on Effective Area

Jinfeng Yu ¹, Lei Zhang,² and Zhi Wang ¹

¹School of Electronics and Information, Yangtze University, Jingzhou, Hubei 434000, China

²College of Computer and Information Technology, Three Gorges University, Yichang, Hubei 443000, China

Correspondence should be addressed to Zhi Wang; 1324385898@qq.com

Received 7 May 2021; Revised 26 May 2021; Accepted 3 June 2021; Published 22 June 2021

Academic Editor: Jin He

Copyright © 2021 Jinfeng Yu et al. This is an open access article distributed under the Creative Commons Attribution License, which permits unrestricted use, distribution, and reproduction in any medium, provided the original work is properly cited.

Iris localization is the most crucial part of the iris processing because its accuracy can directly affect the accuracy of biometric identification in subsequent steps. Yet, the quality of iris images may be sharply degraded due to interference from eyelashes and reflections during image acquisition, which can affect the localization accuracy adversely. To solve the problem, an iris localization algorithm based on effective area is proposed. First, YOLOv4 is used to crop the image to obtain the effective iris area, which is beneficial in improving the accuracy of subsequent localization. Furthermore, a method to remove reflective noise is proposed, which can effectively avoid the problem of noise interference in the process of inner boundary determination. Finally, aiming at the edge deviation caused by eyelashes, an outer boundary adjustment method is proposed. The experimental results show that the proposed method achieves good performance in the localization of iris images of both good quality and noise interference and outperforms other state-of-the-art methods.

1. Introduction

With the rapid development of information security, the role of biometric technology in military, banking, e-commerce, security, and other fields is becoming increasingly more prominent. Among the different technologies available, such as fingerprints, faces, signatures, and the like, iris recognition has gained much attention because of its unique advantages in stability, uniqueness, and universality. As one of the key components of iris recognition systems [1], the purpose of iris localization is to accurately determine the ring area between the pupil and the sclera. However, in practical applications, this process is often accompanied by noise-generated interference, such as eyebrows, blinking, eyelashes, and uneven illumination, which affects the quality of iris images and increases the difficulty of localization, leading to high rates of iris recognition failure.

The integrodifferential operator (IDO) [2, 3], proposed by Daugman, and edge detection combined with the circular Hough transform (CHT) [4], proposed by Wildes, are classic algorithms used in iris localization, which have made great contributions to the research of iris localization. However, the classic algorithms have certain

shortcomings usually: IDO is based on the difference in grayscale of adjacent pixels, so it is extremely sensitive to noise; CHT is based on voting on edge points, and it is difficult to set a universal threshold when the image is marginalized based on gradient information. At the same time, because the two classic algorithms calculate the entire image, it makes the calculation expensive. For these reasons, many scholars have made improvements on the basis of classic algorithms.

In the study by Sun et al. [5], pupil's segmentation according to gray projection and maximum between-class variance method was performed at first, followed by then segmented sector areas in different directions based on the center of the pupil and circle fitting according to the three groups of points with the largest grayscale change in the sector areas. However, this method relies on high-quality images, if there is a lot of noise in the image, the method cannot complete pupil segmentation correctly. In another study [6], a circular Gabor filter [7] was used to estimate the initial pupil center to limit the search range of the iris and pupil circles but did not give a noise solution when using IDO to locate the boundary. Therefore, good results can only be achieved in iris images with less noise.

A morphological method was used in previous studies [8, 9] to remove the reflective noise in the image before binarizing the image. Kumar et al. [8] assumed that the pupil and iris were located in the center of the image, filtered out the binary pixels close to the boundary directly to obtain the largest connected area, then estimated the center of the pupil, and used IDO to determine the iris boundaries finally. They [9] also performed edge detection on binary images, used CHT to locate the inner boundary of the iris, and a limited-angle IDO was used to locate the outer boundary according to the center of the inner boundary. However, method in this study [9] did not consider eyelashes noise.

In the study by Soliman et al. [10], a three-layer threshold system was proposed to solve the binarization problem of images with large differences in grayscale distribution. Then the pupil center was estimated based on the largest connected area and used IDO to accurately locate the boundaries of iris. But there was a problem: when there are large areas of low-gray pixels in the noniris area, the three-layer threshold system will break down. In another study [11], an iris localization method based on rough entropy and circular region analysis was proposed. However, this method is easily susceptible to a localization error of the pupil region because it does not take into account the potential presence of regions with lower gray values than the pupil in the iris image. In the study by Ma et al. [12], a localization method based on conformal geometry was proposed, which was similar to CHT. Firstly, the grayscale values of the whole image were divided into three values (0, 150, and 255) according to the set threshold. Then, the edge detection was performed on the image, and the boundaries of iris was obtained according to the inner product of the edge points in the conformal space. But when the difference in grayscale values of pupil and iris, and background is not obvious, the localization effect of this method is limited. Jan et al. [13] used the bilinear interpolation scheme to remove the reflective noise in image and set the threshold according to continuous low grayscale pixels to binarize the image. Then, the inner boundary of the iris was roughly identified using the largest connected area directly, and the outer boundary was roughly determined using the CHT. Finally, the Fourier series was used to adjust the localization boundaries. However, this method suffered from poor localization for low-quality images.

In recent years, the applications of deep learning in iris localization have gradually attracted researchers' attention. The authors of [14, 15] improved a deep learning network to locate human eyes in binocular images. In the study by Choudhary et al. [16], in order to distinguish living from forged irises, the region of interest (ROI) of the image was obtained using the YOLO [17] network, and a convolutional neural network [18] was used to extract the distinctive texture features. In practical applications, the effective iris area of an eye image usually occupies a small area of the entire image, while other areas are noniris area and can be disregarded, which reduce the localization accuracy of algorithms due to the presence of uneven illumination, hair, eyelids, glasses, and other interference, as shown in Figure 1. If the effective iris area can be accurately extracted, the localization accuracy will be greatly improved. Therefore, in

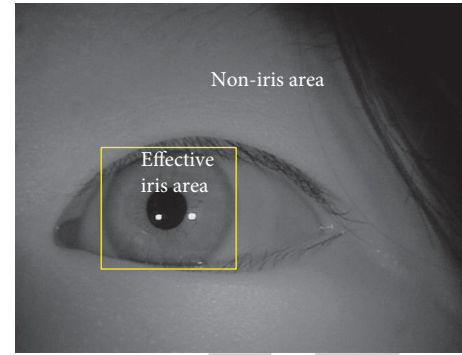


FIGURE 1: Effective iris area and noniris area.

this article, we propose an iris localization algorithm based on effective area. First of all, YOLOv4 [19] is used to crop the image to obtain the effective iris area, which improves the accuracy of subsequent localization. Furthermore, a method to remove reflective noise is proposed, which reduces the interference on the localization of the inner iris boundary. Finally, an outer boundary adjustment method is proposed to improve the accuracy of iris outer boundary localization.

2. Proposed Iris Localization Algorithm

The flowchart of the iris localization method proposed in this article is shown in Figure 2 and includes three parts:

- (1) The effective area of the iris is detected using a YOLOv4 network, and the original image is cropped along the prediction box.
- (2) The minimum grayscale average method [20] is used to binarize the image and roughly estimate the pupil center. A reflective noise removal method is proposed to eliminate the noise interference, while the IDO is used to identify the inner boundary of iris.
- (3) In order to reduce the influence of the sudden grayscale changes in the pupil area and the upper eyelid area while the outer iris boundary is first coarsely identified using the IDO, the pixels around the pupil and the upper eyelid are fused, followed by an outer boundary adjustment method to improve the localization deviation caused by eyelashes.

2.1. Effective Iris Area Extraction using YOLOv4.

Extracting the effective iris area accurately can effectively remove the interference from the noniris area and greatly improve the accuracy of subsequent iris localization. Because of their powerful feature extraction capabilities, existing deep learning algorithms [19, 21] have higher accuracy compared with traditional algorithms in target detection [22–24]. In particular, YOLOv4 uses the CIoU [25] loss function, which considers the distance, overlap rate, scale, and penalty items between the predicted frame and the real frame. It also ensures that the target frame has a more stable regression performance, effectively avoiding the divergence problem in the training process and thus has strong robustness to interference, leading to its excellent performance in target detection tasks.

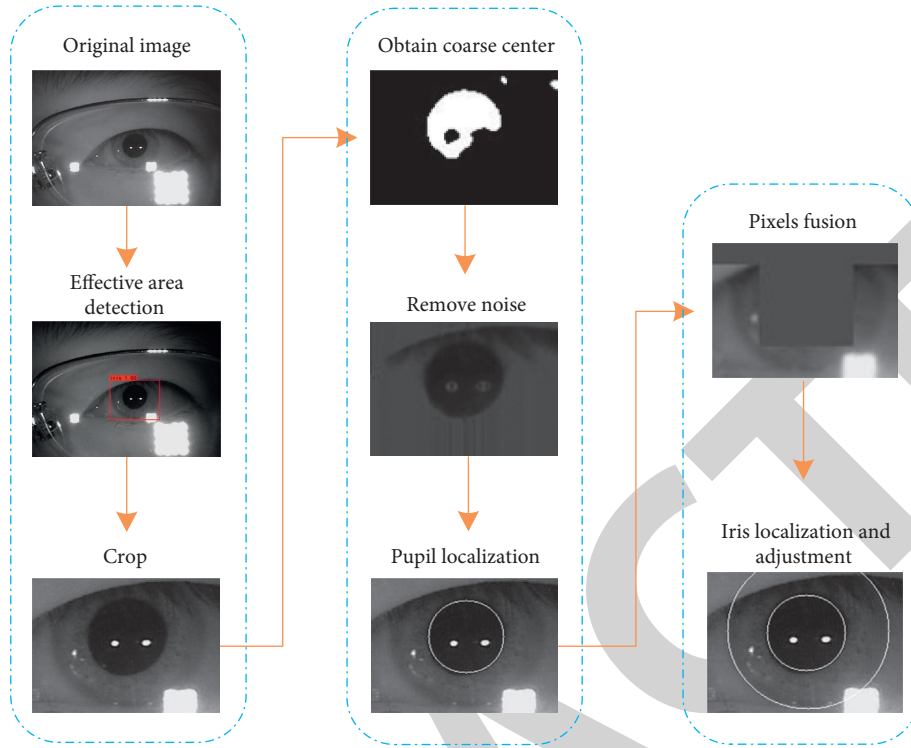


FIGURE 2: Flowchart of proposed iris localization method.

Annotate the effective iris area and use it for training the YOLOv4 model. A trained model is used to predict the effective iris area, and the coordinates of the target with the highest confidence are used to obtain the effective area of iris image. In order to protect the information of iris, the upper and lower borders of the predicted area are expanded by 10 pixels, and the left and right borders are expanded by 20 pixels when cropping. Figure 3(a) shows a prediction example, whereas Figure 3(b) shows the result of the effective iris area extraction.

2.2. Inner Boundary Identification. In the effective iris area, the boundary feature of the pupil (inner boundary of iris) is relatively obvious and easier to identify. Moreover, the successful identification of inner boundary can reduce the difficulty of outer boundary's determination, so the pupil boundary is identified first. A rough estimation of the pupil center based on some prior knowledge can effectively limit the search range of the inner boundary and avoid blindness; hence, we can roughly estimate the location of the pupil center as follows. On the inner boundary between the pupil and the iris, there will usually be an obvious change in the pixels' grayscale values, and the grayscale of the pupil region's pixels that immune to interference will be relatively lower than that of the iris in the effective iris area.

At the same time, the pupil area is vulnerable to reflective noise, so it is necessary to remove the noise before accurate localization using the IDO. Therefore, in this article, we propose a global noise removal method to remove the reflective noise and improve the accuracy of inner boundary localization.

2.2.1. Rough Pupil Center Localization. Inevitably, reflective noise sometimes exists in the effective iris area, which makes the pupil area with low grayscale have high grayscale pixels and affects the traditional methods of coarse localization greatly (such as grayscale projection method and convolution method). Generally speaking, even if there is interference from reflective noise, there will be some normal pixels in the pupil area. Through the adaptive binarization threshold combined with the largest connected area, the minimum grayscale average method [20] can estimate the pupil center successfully. First, we divide the image into $m \times n$ rectangles of equal area according to the size of the effective iris area (Figure 4(a)). Then, we calculate the average grayscale value of each rectangular area and use the minimum average value as the threshold to binarize the image (Figure 4(b)). Finally, we roughly estimate the pupil center and the inner boundary radius from the largest connected area, as shown in equation (1).

$$r_p = \frac{(H + W)}{4},$$

$$x_p = x_{loc} + r_p,$$

$$y_p = y_{loc} + r_p,$$
(1)

where H, W are the height and width of the largest connected area, respectively; (x_{loc}, y_{loc}) are the coordinates of the upper left corner of the largest connected area; (x_p, y_p) is the coarse position of the pupil center, and r_p is the initial radius of the inner boundary.

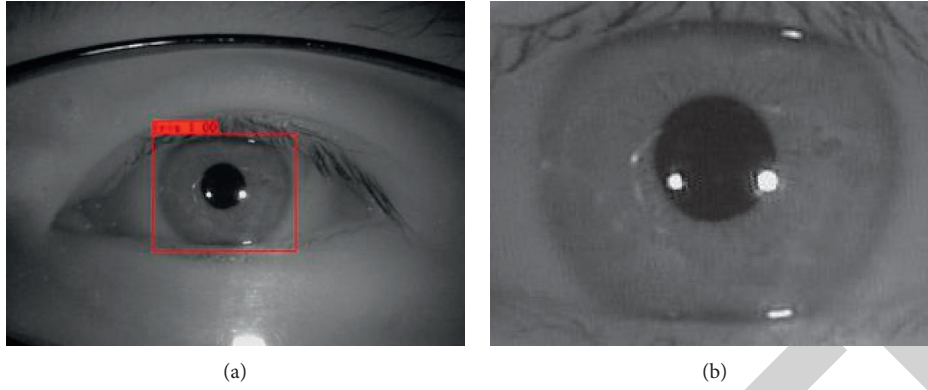


FIGURE 3: Extraction of effective iris area by YOLOv4. (a) Iris area border predicted by YOLOv4. (b) Effective iris area extraction.

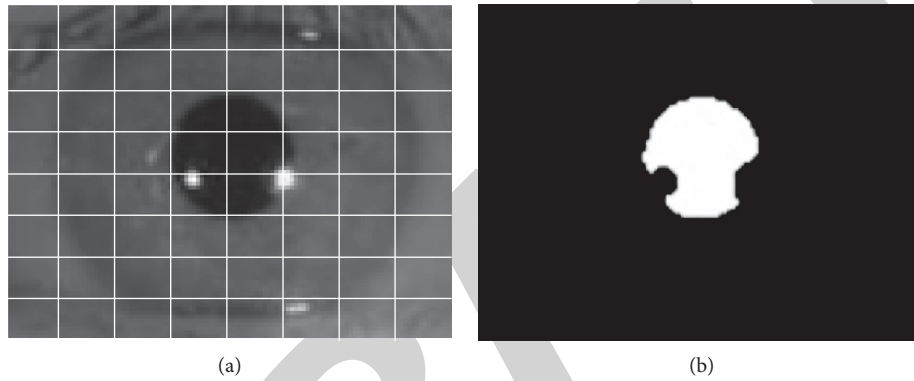


FIGURE 4: Minimum grayscale average method. (a) Division in rectangular areas. (b) Binarization using the minimum average of all areas.

2.2.2. Reflective Noise Removal. The IDO method [2, 3] accumulates the grayscale difference of circumference, and there is no need to set an additional threshold when detecting the circle with grayscale difference, so it has strong adaptability, as shown in equation (2). However, the actual iris image often has reflective noise, which causes the grayscale difference of adjacent pixels to be too large, which greatly restricts the localization accuracy of the IDO method. For this reason, it is necessary to remove the influence of reflective noise before iris localization.

$$\max_{(r, x_0, y_0)} \left| G_\sigma(r) * \frac{\partial}{\partial r} \oint_{r, x_0, y_0} \frac{I(x, y)}{2\pi r} ds \right|, \quad (2)$$

where $G_\sigma(r)$ is the Gaussian smoothing function with a scale of σ ; $*$ represents convolution; r, x_0, y_0 are the integration radius and center, respectively; $I(x, y)$ is the original image of iris.

Existing methods generally use bilinear interpolation [13] or morphological methods [9] to avoid the interference of reflective noise. However, the essence of bilinear interpolation is to select the average grayscale value of four pixels in the vertical and horizontal directions according to a fixed distance to replace the current pixel, so it is susceptible to the interpolation distance when performing reflective noise filtering. If the distance is too small, the noise cannot be completely removed, while too large values may affect the effective boundary of the iris adversely. During reflective

noise removal, morphological methods commonly damage the effective boundary of the iris due to the difficulty of setting the grayscale value for hole filling.

Even when affected by reflective noise, the normal pixels' grayscale value of the pupil area is lower than the average grayscale value of the entire iris area. For this reason, in this article, we propose a method of removing reflective noise based on global characteristics. First, we calculate the average grayscale value of the entire iris image as the global threshold, and use this as the basis for replacing the reflective noise. In view of the fact that the IDO is only sensitive to arc-shaped grayscale mutations, pixel replacement is performed on the square area with the coarse localization center of the pupil as the center point and a side length q column by column (that is, the area where the inner boundary of the iris may appear). If the current pixel is greater than the threshold, the pixel is judged as a reflective noise pixel, and it is replaced with the nearest effective pixel's grayscale value in the same column. Otherwise, the original pixel as the valid pixel is retained, and its grayscale value is stored. The replacement result is shown in Figure 5(a). On the one hand, the proposed method takes into account the global characteristics of pixels, which can better eliminate the interference of reflective noise. On the other hand, it can better retain the effective iris edge by replacing the reflective noise pixel value with an acceptable effective pixel's grayscale value

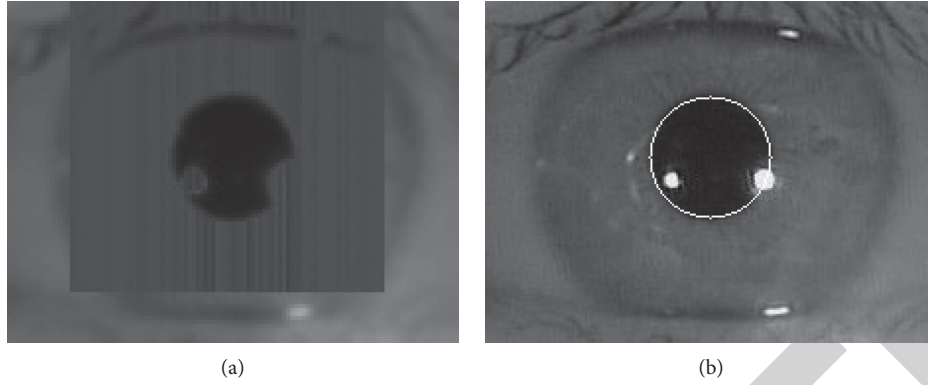


FIGURE 5: Localization of inner boundary. (a) Reflective noise removal. (b) Precise localization of inner boundary.

Input: The obtained effective iris area, img ; The first and last columns of the noise filled area, L_c and R_c ; The first and last rows of the noise filled area, U_r and D_r ;

Output: The image after reflective noise removal

```
(1) import numpy as np
(2)  $T_i = np.mean(img)$  #calculate the average grayscale value of the image
(3)  $B_{uff} = T_i$ 
(4) for  $j$  in range ( $L_c, R_c$ ):
(5)     for  $i$  in range ( $U_r, D_r$ ):
(6)          $P_{ix} = img[i][j]$ 
(7)         if  $P_{ix} > T_i$ : #is the current pixel a valid pixel?
(8)              $img[i][j] = B_{uff}$ 
(9)         else:
(10)             $B_{uff} = P_{ix}$ 
(11) return  $img$ 
```

ALGORITHM 1: Pseudo code of reflective noise removal.

(i.e. below the threshold and nearest on the same column). The pseudo code of the reflective noise removal is shown in Algorithm 1.

2.2.3. Identification of Inner Boundary. The inner boundary is identified by follows:

- According to the pupil center (x_p, y_p) roughly estimated by the minimum grayscale average method, the search range of the inner boundary center is limited to a square area with the rough pupil center as the center point and a side length p . The value of p should ensure that the true inner boundary center of the iris can be located.
- Using the reflective noise removal method proposed in this article to remove the reflective noise in the area where the inner boundary of the iris may appear, and the area is set as a square area with the rough pupil center as the center point and a side length q . In this article, q is set according to the rough pupil center and the maximum radius of the inner boundary.
- Setting the radius range of the inner boundary (r_{p1}, r_{p2}) , where r_{p1} is the initial radius of the inner boundary estimated by the minimum grayscale average method, and r_{p2} is set according to the long

side of the effective iris area. Then, we obtain the inner boundary center (X_p, Y_p) and radius R_p using the IDO, and the localization result is shown in Figure 5(b).

2.3. Determination of Outer Boundary. The outer boundary of the iris refers to the boundary between the iris and the sclera, which is not always visible and may be occluded by the eyelid or eyelashes and affected by other types of noise. Therefore, the upper eyelid and the pupil regions are fused before boundary identification, so as to reduce the problem of the sudden grayscale changes caused by pupil and eyelashes effectively while using the IDO to identify the outer boundary. At the same time, for our eyes, the pupil is surrounded by the iris, so the center of the outer boundary can be defined according to the center of the inner boundary.

2.3.1. Regional Pixel Fusion. In order to reduce the influence of the inner boundary, as well as the problems of eyelashes and occlusion by the upper eyelid, the pupil region and upper eyelid are fused when identifying the outer boundary of the iris. The details are as follows. First, a pixel matrix in the lower right corner of the iris image is selected according to the center and radius of the acquired inner boundary and

its average grayscale value is calculated (a relatively mild grayscale value is needed to reduce sudden changes in grayscale leading to localization failure). Then, the pixels of the pupil region and the upper eyelid are replaced according to the iris inner boundary parameters. The pseudo code of the regional pixel fusion is shown in Algorithm 2, and the fusion result is shown in Figure 6(a).

2.3.2. Outer Boundary Adjustment. When the iris area occupies a small proportion of the overall image, the localization deviation of outer boundary caused by the eyelashes in existing algorithms is often difficult to detect, although the determined boundary does not fit the actual boundary accurately. Therefore, it is necessary to adjust the outer boundary of the iris to avoid localization deviation that affect the subsequent recognition results. The inaccurate outer boundary caused by eyelashes results in imperfect iris boundary fitting. So, in the area without eyelash interference (the lower part of the outer boundary), the grayscale difference between adjacent pixels in the same radial direction is small. Therefore, we can select several sets of IDO parameters with larger circumferential difference values to perform outer boundary comparison in areas with less eyelash interference and choose the optimal circle parameter. To this end, in this article, we propose an outer boundary adjustment method, as follows:

- (a) The parameters acquired by IDO are composed of radius and center, and only a set of parameters with the largest grayscale difference value on circumference are retained. We keep z sets of IDO parameters with the largest difference values and compare them according to certain rules.
- (b) Take the center of the circle as the center and make rays according to certain angles direction. The intersection points of the rays and the circle with angles of 0° , -20° , and -30° are a_1 , b_1 , and c_1 , and the intersection points of the rays and the circle with angles of 180° , 200° , and 210° are a_2 , b_2 , and c_2 .
- (c) We extend the radius of the circle by Δn pixels and obtain the intersection points of the rays in the original angle's direction and the circle a_3 , b_3 , c_3 and a_4 , b_4 , c_4 , as shown in Figure 6(b).
- (d) Calculating the grayscale difference of two pixels in the same angle direction and getting the accumulated value. Because of the grayscale difference between the iris and the sclera, the accumulated value will be larger while the outer boundary fits well enough. Then, the optimal circle parameters is obtained by comparing the accumulated values. The pseudo code of the outer boundary adjustment is shown in Algorithm 3.

2.3.3. Determination of Outer Boundary. The outer boundary is determined by follows:

- (a) According to the identified inner boundary's center (X_p, Y_p) and radius R_p , we remove the interference of

pupil and upper eyelid through strategy of regional pixel fusion while determining the outer boundary and limit the outer boundary center within the square area centered at the center point of the inner boundary and with a side length of k (the area where the center of outer boundary may appear).

- (b) In order to further remove the interference of eyelids, the IDO's integration angle is limited between $(-45^\circ, 30^\circ)$ and $(150^\circ, 225^\circ)$ [8], as shown in Figure 6(c). Setting the outer boundary radius range to $(R_p, 5R_p)$ according to the radius of inner boundary. Then, we keep z sets of IDO parameters with the largest difference values on circumference.
- (c) Comparing the z sets of IDO parameters according to the outer boundary adjustment method proposed in this article, the optimal outer boundary parameters (X_I, Y_I, R_I) are obtained to adjust the localization deviation caused by eyelashes. Figure 6(d) shows the final boundary determination result.

3. Experimental Results

The experimental environment of this study is shown in Table 1. Select 3000 images from CASIA-IrisV4-thousand and 1000 images from CASIA-IrisV3-Interval to label the training set of YOLOv4 model. The software used to label the effective iris area was LabelImg, shown in Figure 7.

In order to verify the effectiveness of the improved algorithm, comparative experiments were carried out to determine whether the use of YOLOv4 to extract the effective iris area aids the proposed iris localization method, the effect of reflective noise removal, and that of outer boundary adjustment. At the same time, in order to verify the performance of the proposed algorithm, we compared with other excellent iris localization methods [8, 10, 13]. The algorithm parameters were set as follows: The area where the center of the inner boundary may appear was set as a square with a side length of $p=100$, the maximum radius of the inner boundary r_{p2} was set to one-third of the long side of the effective iris area, the side length q of the reflective noise removing range was the sum of the inner boundary center range and the inner boundary diameter, and the center range of the outer boundary was $k=20$. The sets of the IDO parameters reserved was $z=3$, the extend distance of radius $\Delta n=2$. We randomly selected 2000 images from each of CASIA-IrisV4-thousand and CASIA-IrisV3-Interval data sets for localization. In this article, the localization accuracy on the corresponding data set is used as the evaluation index:

$$\text{Acc} = \frac{N_s}{N_t} \times 100\%, \quad (3)$$

where N_s refers to the number of images accurately located, and N_t is the total number of images.

3.1. Effective Iris Area Extraction Using YOLOv4. In order to verify the effectiveness of extracting the effective iris area using YOLOv4, comparative experiments are carried out. The purpose of the experiments was to determine whether the use

Input: The obtained effective iris area, IMG ; The center of the inner boundary, (X_p, Y_p) ; the radius of the inner boundary, R_p ;
Output: The image after regional pixel fusion **1 import** math **2** $Pix_block = IMG[(Y_p + R_p - 1): (Y_p + R_p + 1), (X_p + R_p + 4): (X_p + R_p + 6)]$ #get pixel matrix
 (3) $p_a, p_b, p_c, p_d = Pix_block [0] [0], Pix_block [0] [1], Pix_block [1] [0], Pix_block [1] [1]$
 (4) $P_aver = \text{math.floor} (p_a/4 + p_b/4 + p_c/4 + p_d/4)$ # calculate the average grayscale value
 (5) $IMG [Y_p - R_p - 5: Y_p + R_p + 5, X_p - R_p - 5: X_p + R_p + 5] = P_aver$ #fuse the pupil
 (6) $IMG [0: Y_p - R_p, :] = P_aver$ #fuse the upper eyelid
 (7) **return** IMG

ALGORITHM 2: Pseudo code of regional pixel fusion.

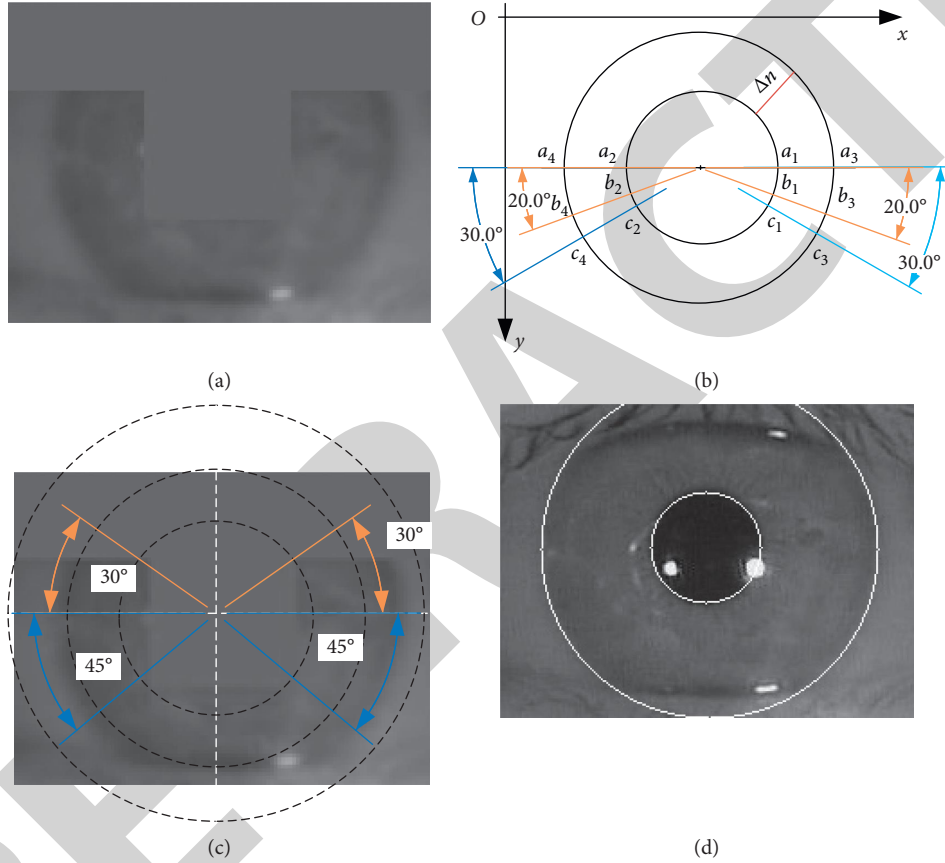


FIGURE 6: Determination of outer boundary. (a) Regional pixels fusion. (b) Outer boundary adjustment. (c) Integral angle limits. (d) Boundary determination result.

Input: The z sets of IDO parameters with the largest difference values, $para_1, para_2, \dots, para_z$; the pixels in six directions were obtained according to each set of parameters, $a_{1i}, a_{2i}, a_{3i}, a_{4i}, b_{1i}, b_{2i}, b_{3i}, b_{4i}, c_{1i}, c_{2i}, c_{3i}, c_{4i}$, where $i = 1, 2, \dots, z$;
Output: The optimal parameters, Opt_para ;
 (1) $Para = (para_1, para_2, \dots, para_z)$
 (2) $val_1 = (a_{11} - a_{31})^2 + (a_{21} - a_{41})^2 + (b_{11} - b_{31})^2 + (b_{21} - b_{41})^2 + (c_{11} - c_{31})^2 + (c_{21} - c_{41})^2$
 (3) $val_2 = (a_{12} - a_{32})^2 + (a_{22} - a_{42})^2 + (b_{12} - b_{32})^2 + (b_{22} - b_{42})^2 + (c_{12} - c_{32})^2 + (c_{22} - c_{42})^2$
 (4) ...
 (5) $val_z = (a_{1z} - a_{3z})^2 + (a_{2z} - a_{4z})^2 + (b_{1z} - b_{3z})^2 + (b_{2z} - b_{4z})^2 + (c_{1z} - c_{3z})^2 + (c_{2z} - c_{4z})^2$
 (6) $Value = [val_1, val_2, \dots, val_z]$
 (7) $Index = Value.index (\max (Value))$ #get the index of maximum
 (8) $Opt_para = Para [Index]$
 (9) **return** Opt_para

ALGORITHM 3: Pseudo code of outer boundary adjustment.

TABLE 1: Experimental environment.

| Environment | Configuration |
|-------------------------|------------------------|
| Operating system | Ubuntu16.04 |
| GPU | NVIDIA GeForce RTX2080 |
| GPU RAM | 8 Gb |
| CPU | Core i7 |
| RAM | 16 Gb |
| Programming environment | Python 3.7 |

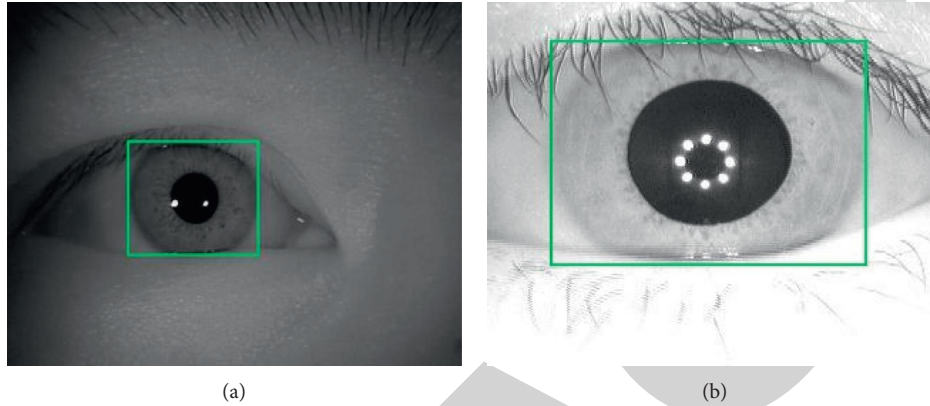


FIGURE 7: Training set labeling. (a) Labeling a CASIA-IrisV4-thousand image. (b) Labeling a CASIA-IrisV3-Interval.

of YOLOv4 to extract the effective iris area aids the iris localization method proposed in this article. The comparative experimental results are shown in Table 2 and Figure 8.

As shown in Table 2, after using YOLOv4 to extract the effective iris area in CASIA-IrisV4-thousand data set, the iris localization accuracy was greatly improved. It can be seen from Figure 8(b) that when the effective iris area is not extracted using YOLOv4, the pupil region may not be the area of lowest grayscale because of the black area around the image of the human eye. This results in an error when using the grayscale levels directly to roughly estimate the center of the pupil, which in turn leads to the wrong determination of the iris boundary to the upper right corner of the image. From Figure 8(c), we see that when YOLOv4 is used to extract the effective iris area, there are fewer invalid pixels interfering with the pupil center estimation process, so the localization accuracy is greatly improved. The above experimental results verify the effectiveness of extracting the effective area of the iris using YOLOv4.

3.2. Reflective Noise Removal. In order to verify the effectiveness of the strategy of reflective noise removal proposed in this article, a comparative experiment is carried out to determine whether the reflective noise removal method proposed aids the iris localization accuracy. The comparison results are shown in Table 3 and Figure 9.

As shown in Table 3, after the removal of reflective noise points, the localization accuracy was improved to a certain extent in both data sets. As can be seen from Figure 9(b), when there is reflective noise in the effective area of the iris, the grayscale levels of the pupil area are lower, while the grayscale levels of the reflective noise are higher in general. If

TABLE 2: Comparison of proposed iris localization accuracy with and without YOLOv4 to extract the effective iris area.

| YOLOv4-crop | CASIA-IrisV4-thousand (%) | CASIA-IrisV3-interval (%) |
|-------------|---------------------------|---------------------------|
| No | 39.80 | 97.15 |
| Yes | 98.60 | 98.85 |

the reflective noise is not removed, the application of IDO for difference accumulation is adversely affected, and this eventually results in localization error. It can be seen from Figure 9(c) that removing the reflective points under the condition of protecting the effective edges can reduce the impact of reflective noise on the inner boundary localization effectively and ultimately improve the localization accuracy. The experimental results verify the effectiveness of the proposed reflective noise removal strategy.

3.3. Outer Boundary Adjustment. In order to verify the effectiveness of the proposed outer boundary adjustment method, a comparative experiment was carried out to determine whether the adjustment improves the accuracy of the iris localization method proposed in this article. The comparative experiment results are shown in Table 4 and Figure 10.

As indicated in Table 4, the outer boundary adjustment method can improve the localization accuracy to a certain extent. In the case shown in Figure 10(b), there are dense eyelashes in the upper eyelid area, and many long eyelashes cover the upper part of the outer boundary after extracting the effective iris area. This makes the grayscale difference of the eyelashes more obvious than that of the true outer boundary of the iris and results in a slight deviation in the

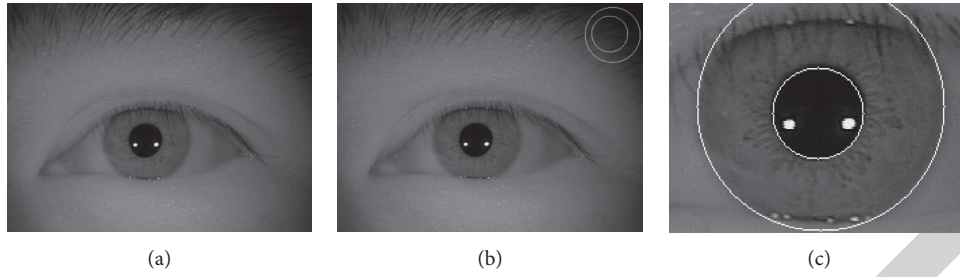


FIGURE 8: Iris localization result without and with YOLOv4 to extract effective iris area. (a) Original image. (b) Localization without YOLOv4. (c) Localization with YOLOv4.

TABLE 3: Comparison of localization accuracy between without and with reflective noise removal.

| Noise removal | CASIA-IrisV4-thousand (%) | CASIA-IrisV3-interval (%) |
|---------------|---------------------------|---------------------------|
| No | 86.40 | 96.10 |
| Yes | 98.60 | 98.85 |

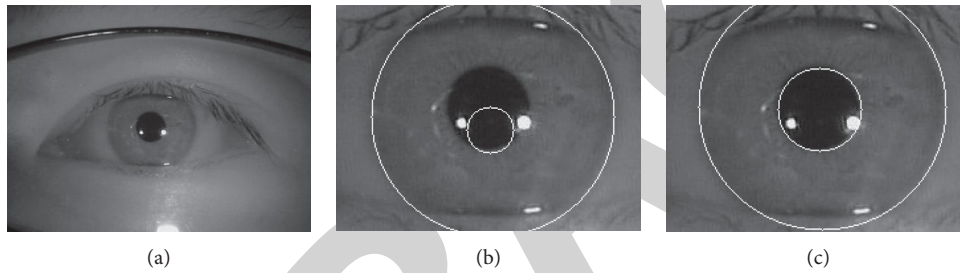


FIGURE 9: Iris localization result without and with reflective noise removal. (a) Original image. (b) Localization without reflective noise removal. (c) Localization with reflective noise removal.

TABLE 4: Comparison of localization accuracy without and with outer boundary adjustment.

| Adjustment | CASIA-IrisV4-thousand (%) | CASIA-IrisV3-interval (%) |
|------------|---------------------------|---------------------------|
| No | 98.40 | 98.70 |
| Yes | 98.60 | 98.85 |

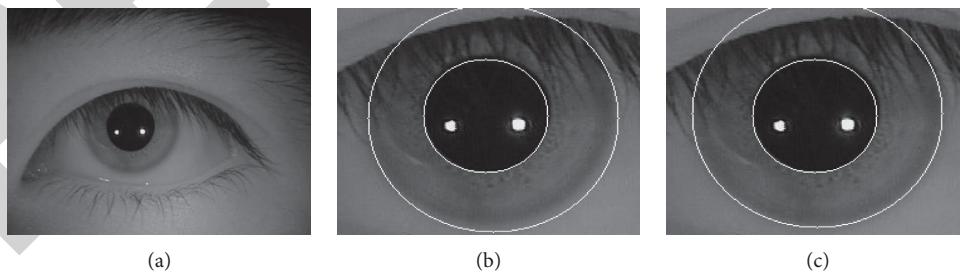


FIGURE 10: Iris localization result without and with outer boundary adjustment. (a) Original image. (b) Localization without adjustment. (c) Localization with adjustment.

determination of the outer boundary. At the same time, because the deviating outer boundary of the iris does not correspond to the actual boundary, the radial grayscale difference value at the lower part of the outer boundary of the iris is small. It can be seen from Figure 10(c) that the localization error caused by long eyelashes is adjusted

effectively through the radial difference comparison of several groups of parameters with the largest integral value obtained via IDO, and the iris localization accuracy is ultimately improved. The above experimental results verify the effectiveness of the proposed outer boundary adjustment method.

TABLE 5: Comparison of localization accuracy of several algorithms.

| Method | CASIA-IrisV4-thousand (%) | CASIA-IrisV3-interval (%) |
|---------------------|---------------------------|---------------------------|
| Kumar et al. [8] | 97.95 | 98.30 |
| Soliman et al. [10] | 94.60 | 97.95 |
| Jan et al. [13] | 94.00 | 96.65 |
| Proposed | 98.60 | 98.85 |

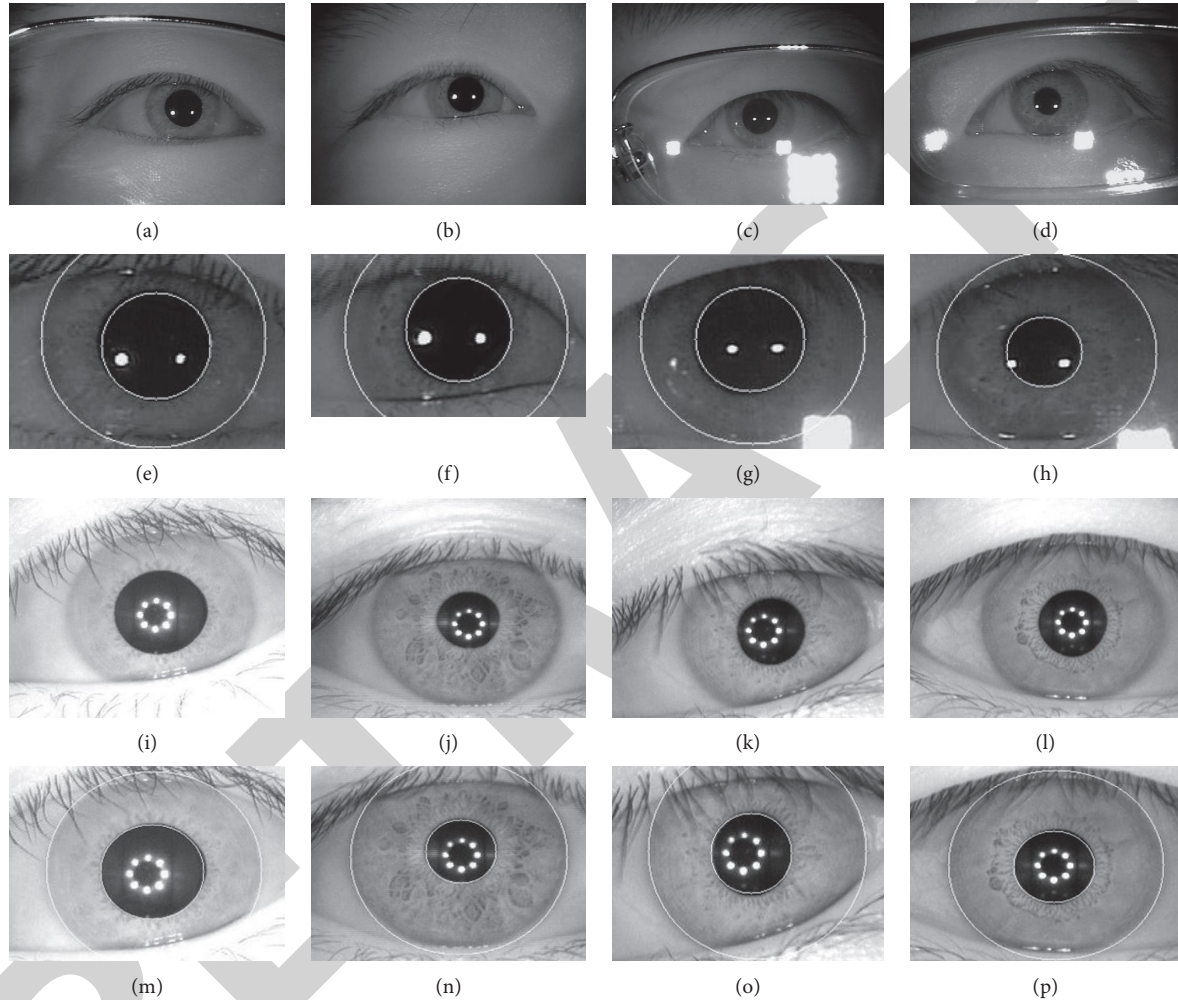


FIGURE 11: Examples of the iris localization results of the proposed algorithm.

3.4. Comparison with Other Algorithms. In order to verify the performance of the proposed algorithm, we compared it with the algorithms presented in the literature [8, 10, 13]. All algorithms completed localization based on the effective iris area extracted by YOLOv4. The experimental results are shown in Table 5 and Figure 11. The first and second lines of Figure 11 are partial CASIA-IrisV4-thousand images and their iris localization results, while the third and the fourth lines are partial CASIA-IrisV3-Interval images and their localization results.

As can be seen from Table 5, the proposed method has better results when compared with other localization methods. As can be seen from Figure 11, when the iris area

accounts for a small proportion of the whole image, there is a lot of interference in the image, and the proposed algorithm can effectively remove the interference caused by the eyeglass frame, reflections, the eyebrows, hair, etc. and obtain the effective iris area to achieve accurate localization. The quality of images is higher when the iris area accounts for a large proportion of the whole image, and the proposed algorithm still yields better performance than other state-of-the-art methods. At the same time, the proposed method also suffers localization errors when the iris area is severely obscured, which shows that this method has some room for improvement when the effective edges are fewer.

4. Conclusion

Aiming at the problem that actual iris images suffer from a variety of noise elements, which lead to the reduction of localization accuracy, in this article, we proposed an iris localization algorithm based on effective area. First, in order to enhance the accuracy of the ensuing localization, the YOLOv4 model is introduced to crop the iris image and obtain the effective region of the iris. Furthermore, a method to remove reflective noise is proposed, which avoids the problem of determining the inner iris boundary in the presence of noise interference effectively. Finally, an improved radial difference adjustment method is proposed to improve the accuracy of outer iris boundary localization. The proposed method achieved good performance in iris localization in images of good quality and with noise interference.

Data Availability

The data were taken from Chinese Academy of Sciences' Institute of Automation (CASIA) iris databases.

Conflicts of Interest

The authors declare that they have no conflicts of interest.

References

- [1] G. Gautam and S. Mukhopadhyay, "Challenges, taxonomy and techniques of iris localization: a survey," *Digital Signal Processing*, vol. 107, Article ID 102852, 2020.
- [2] J. G. Daugman, "High confidence visual recognition of persons by a test of statistical independence," *IEEE Transactions on Pattern Analysis and Machine Intelligence*, vol. 15, no. 11, pp. 1148–1161, 1993.
- [3] J. Daugman, "How iris recognition works," *IEEE Transactions on Circuits and Systems for Video Technology*, vol. 14, no. 1, pp. 21–30, 2004.
- [4] R. P. Wildes, "Iris recognition: an emerging biometric technology," *Proceedings of the IEEE*, vol. 85, no. 9, pp. 1348–1363, 1997.
- [5] Z. Sun, Z. Chen, and X. Li, "Iris location algorithm based on method of gray value of unit sector area," *Optical Technique*, vol. 45, no. 2, pp. 228–233, 2019, In Chinese.
- [6] A. Radman, K. Jumari, and N. Zainal, "Iris segmentation in visible wavelength environment," *Procedia Engineering*, vol. 41, pp. 743–748, 2012.
- [7] J. Zhang, T. Tan, and L. Ma, "Invariant texture segmentation via circular Gabor filters," *Object recognition supported by user interaction for service robots*, vol. 2, pp. 901–904, 2002.
- [8] V. Kumar, A. Asati, and A. Gupta, "Iris localization based on integro-differential operator for unconstrained infrared iris images," in *Proceedings of the 2015 International Conference on Signal Processing, Computing and Control (ISPCC)*, pp. 277–281, Pacific Grove, CA, USA, November 2015.
- [9] V. Kumar, A. Asati, and A. Gupta, "An iris localization method for noisy infrared iris images," in *Proceedings of the 2015 IEEE International Conference on Signal and Image Processing Applications (ICSIPA)*, pp. 208–213, Kuala Lumpur, Malaysia, October 2015.
- [10] N. F. Soliman, E. Mohamed, F. Magdi, and F. E. A. El-Samie, "Efficient iris localization and recognition," *Optik*, vol. 140, pp. 469–475, 2017.
- [11] M. Sardar, S. Mitra, and B. Uma Shankar, "Iris localization using rough entropy and CSA: a soft computing approach," *Applied Soft Computing*, vol. 67, pp. 61–69, 2018.
- [12] L. Ma, H. Li, and K. Yu, "Fast iris localization algorithm on noisy images based on conformal geometric algebra," *Digital Signal Processing*, vol. 100, Article ID 102682, 2020.
- [13] F. Jan, N. Min-Allah, S. Agha et al., "A robust iris localization scheme for the iris recognition," *Multimedia Tools and Applications*, vol. 80, pp. 1–27, 2020.
- [14] T. Tong, W. Shen, and Y. Mao, "Multi-task iris fast location method based on cascaded neural network," *Computer Engineering and Applications*, vol. 56, no. 12, pp. 118–124, 2020, In Chinese.
- [15] J. Chen and W. Shen, "Human eye localization and classification algorithm based on EL-YO," *Computer Engineering and Applications*, vol. 1–11, 2021, <http://kns.cnki.net/kcm%20s/detail/11.2127.TP.20200820.1000.008.html> In Chinese.
- [16] M. Choudhary, V. Tiwari, and V. Uduthalappally, "Iris presentation attack detection based on best-k feature selection from YOLO inspired RoI," *Neural Computing and Applications*, vol. 33, pp. 1–21, 2020.
- [17] J. Redmon, S. Divvala, R. Girshick et al., "You only look once: unified, real-time object detection," in *Proceedings of the IEEE Conference on Computer Vision and Pattern Recognition*, pp. 779–788, Las Vegas, NV, USA, June 2016.
- [18] K. Kang, W. Ouyang, H. Li et al., "Object detection from video tubelets with convolutional neural networks," *Proceedings of the IEEE Conference on Computer Vision and Pattern Recognition*, pp. 817–825, Las Vegas, NV, USA, June 2016.
- [19] A. Bochkovskiy, C. Y. Wang, and H. Y. M. Liao, "Yolov4: optimal speed and accuracy of object detection," 2020, <https://arxiv.org/abs/2004.10934>.
- [20] Y. Ma, L. Zhou, and L. Yuan, "Iris location algorithm by vector field convolution," *Infrared and Laser Engineering*, vol. 43, no. 10, pp. 3497–3503, 2014, In Chinese.
- [21] J. Redmon and A. Farhadi, "Yolov3: an incremental improvement," 2018, <https://arxiv.org/pdf/1804.02767.pdf>.
- [22] S. Ren, K. He, R. Girshick et al., "Faster R-CNN: towards real-time object detection with region proposal networks," *IEEE Transactions on Pattern Analysis and Machine Intelligence*, vol. 39, no. 6, 2015.
- [23] K.-M. He, G. Gkioxari, P. Dollár et al., "Mask r-cnn," in *Proceedings of the IEEE International Conference on Computer Vision*, pp. 2961–2969, Venice, Italy, October 2017.
- [24] N. Dalal and B. Triggs, "Histograms of oriented gradients for human detection," in *Proceedings of the IEEE Computer Society Conference on Computer Vision & Pattern Recognition*, vol. 1, pp. 886–893, San Diego, CA, USA, June 2005.
- [25] Z. Zheng, P. Wang, W. Liu et al., "Distance-IoU loss: faster and better learning for bounding box regression," *Proceedings of the AAAI Conference on Artificial Intelligence*, vol. 34, no. 7, pp. 12993–13000, 2020.